Large Faraday effect of borate glasses with high Tb^3 content prepared by containerless processing

AUTHOR(S):

Suzuki, Futoshi; Sato, Fumio; Oshita, Hiroyuki; Yao, Situ; Nakatsuka, Yuko; Tanaka, Katsuhisa

CITATION:

Suzuki, Futoshi ...[et al]. Large Faraday effect of borate glasses with high Tb^3 content prepared by containerless processing. Optical Materials 2018, 76: 174-177

ISSUE DATE:

2018-02

URL:

http://hdl.handle.net/2433/235676

Large Faraday effect of borate glasses with high Tb^{3+} content prepared by containerless processing

Futoshi Suzuki[1*], Fumio Sato[1], Hiroyuki Oshita[1], Situ Yao[2], Yuko Nakatsuka[2], Katsuhisa Tanaka[2]

1. Nippon Electric Glass Co., Ltd., 7-1, Seiran 2-Chome, Otsu, Shiga 520-8639, Japan
2. Department of Material Chemistry, Graduate School of Engineering, Kyoto University, Nishikyo-ku, Kyoto 615-8510, Japan

*Corresponding author.
E-mail address: fsuzuki@neg.co.jp

Abstract

Borate glasses containing a large amount of Tb^{3+} ions have been prepared by containerless processing. The content of Tb_2O_3 reached 60 mol%. The glass bearing the highest content of Tb^{3+} ions showed a large Faraday effect; the Verdet constant was 234 rad/T m. Annealing of the glasses in H_2/N_2 atmosphere resulted in a low optical absorption coefficient, leading to an extremely large magneto-optical figure of merit that was ~1.7 times higher than that of $Tb_3Ga_5O_{12}$ single crystal.

Keywords: Faraday rotation, Oxide glass, Containerless processing

1. Introduction

The Faraday effect is one of the magneto-optical phenomena, that is, a rotation of the polarization plane of linearly polarized light that takes place when the light passes through a material in a magnetic field or ferro- and ferrimagnets. Materials with a large Faraday effect have been used as optical isolators, optical circulators, and sensors of electrical current or magnetic fields.

It is well known that garnet-type rare-earth ferrite crystals such as $Y_3Fe_5O_{12}$ (YIG), $Gd_3Fe_5O_{12}$, and $Bi_3Fe_5O_{12}$ exhibit an extremely large Faraday effect and are highly transparent to infrared light [1-6]. Therefore, the garnet-type ferrites have been practically utilized in the infrared range, for example, around a wavelength of 1550 nm, which is suitable for optical telecommunications. However, these ferrite crystals have rather intense optical absorption in the wavelength range below 1100 nm.

Recently, short-wavelength lasers typified by He-Ne lasers, laser diodes, and fiber lasers have been widely utilized for sensing, medical applications, and laser processing, for example. Optical isolators are an important element for laser systems. Thus, the demand for magneto-optical materials with both a large Faraday effect and high transparency in the visible to near-infrared (vis-NIR) region is steadily increasing.

The Faraday effect of paramagnetic materials is generally evaluated by the relation, $\theta_F = VHL$, where θ_F is the Faraday rotation angle, H is the external magnetic field, L is the length of the light pass in the material, and V is the Verdet constant for the material. Currently, terbium gallium garnet ($Tb_3Ga_5O_{12}$, TGG) is the most widely used as a magneto-optical material in the visible range. TGG is highly transparent in the visible range and its Verdet constant is ~134 rad/T m at 633 nm [7].

On the other hand, many studies have been carried out on the Faraday effect of rare-earth-containing glasses, because in general, glasses provide the advantages of tunable optical and mechanical properties by adjusting the chemical composition and controlling the shape of the product such as a plate, rod, or fiber [8-17]. Among the rare-earth ions, Tb^{3+} shows few optical absorption lines in a wide wavelength range from 400 to 1500 nm. Moreover, the large magnetic moment of the Tb^{3+} ion is fairly effective in generating a large Faraday effect. To achieve a large magneto-optical figure of merit as well as a large Faraday effect, it is important to incorporate a large amount of Tb^{3+} ions in glasses. However, it is not easy to avoid crystallization in the preparation of the glasses containing a high content of Tb^{3+} ions when the conventional melt-quenching method is employed with a crucible as a container for the melt. One way of circumventing the crystallization issue is to perform containerless processing, which has recently attracted attention as an emerging glass-preparing method. This method enables the vitrification of materials in bulk form even if they have low glass-forming ability, because there is no contact with the container wall where heterogeneous nucleation occurs. Recently, glass formation through containerless processing has been performed for glass systems such as BaO-TiO_2, La_2O_3-TiO_2, La_2O_3-Nb_2O_5, and La_2O_3-WO_3 [18-21]. It is expected that glasses containing a high content of Tb_2O_3 can also be prepared by containerless processing.

In this research, we aim at the preparation of oxide glasses containing a large amount of Tb^{3+} to realize a magneto-optical material with a Verdet constant larger than that of a TGG single crystal and high transparency in the vis-NIR region.

2. Experimental procedure

Borate glasses containing a large amount of Tb_2O_3 (Tb_2O_3 concentrations of 45, 55, and 60 mol%) were prepared by containerless processing. Hereafter, these glasses are simply referred to as 45T, 55T, and 60T. Powders of reagent-grade Tb_4O_7, B_2O_3, SiO_2, and Al_2O_3 were weighed and mixed to obtain the designed proportions. The mixture of powders was placed on the nozzle of an aerodynamic levitation (ADL) furnace and levitated by nitrogen gas flow. The flow rate was monitored and controlled by a mass-flow meter. A high-resolution charge-coupled device (CCD) video camera equipped with telephoto objective lens was used to observe a magnified view of the samples. A CO_2 laser was used to melt the levitated sample and its temperature was measured by a pyrometer. The levitated melt was rapidly cooled to room temperature and solidified by turning off the laser.

The glass transition temperature (T_g) and crystallization temperature (T_c) were determined by differential thermal analysis (DTA) at a heating rate of 10 °C/min. Vitrified samples were annealed at their glass transition temperatures in 4%-H_2/96%-N_2 atmosphere for 10 h to reduce Tb^{4+} to Tb^{3+} then cooled slowly to release the thermal stress. The density of the glasses was measured by the Archimedes method. The transmittance spectra of glass plates 1 mm thick were obtained in the wavelength range of 300-1200 nm using a UV-vis spectrometer. The wavelength variation of the Faraday rotation angle was measured at room temperature by using a commercial measurement system for the Faraday and Kerr effects (Model K-250, JASCO). The light source was Xe lamp and the external magnetic field was 1.5 T.

3. Results and discussion

3.1. Transmittance

Glass spheres with a diameter of approximately 5 mm were prepared using an aerodynamic levitation furnace. Before annealing, the glass samples had brown color. After annealing at T_g in 4%-H_2/96%-N_2 atmosphere, they became colorless. Figure 1 depicts the transmittance spectra of 60T before and after annealing. For

comparison, the spectrum of a TGG single crystal (made by the Czochralski method, CASTECH Inc.) is also shown. In the spectrum of 60T before annealing, a broad optical absorption band can be seen at wavelengths shorter than 900 nm. The absorption is ascribable to the Tb^{4+} ion [22].

The spectra of 60T after annealing and TGG have similar absorption peaks at around 300-400 nm and ~480 nm. The absorption peaks corresponds to $^7F_6 \rightarrow {}^5H_7$, $^5L_9$, $^5D_3$, and $^5D_4$ transitions of the Tb^{3+} ion. It is considered that almost all the terbium ions in 60T are present as Tb^{3+} after the annealing, as suggested by the high similarity between the profiles of the spectra of the 60T glass after annealing and the TGG single crystal.

3.2. Faraday effect

Figure 2 illustrates the wavelength dependence of the Verdet constant at room temperature for 45T, 55T, 60T, and the TGG crystal. The Verdet constant is negative in the wavelength range studied, indicating that the Faraday rotation is caused by paramagnetic Tb^{3+} ions. The Verdet constant tends to increase with decreasing wavelength. Furthermore, all the glass samples have a larger Verdet constant than TGG in the entire wavelength range.

The density, Tb^{3+} ion concentration, and Verdet constant at 633 nm for each sample are summarized in Table 1, and the dependence of the Verdet constant at 633 nm on the Tb^{3+} ion concentration is shown in Fig. 3. It can be seen that the Verdet constant increases almost linearly with increasing Tb^{3+} ion concentration. A similar tendency was also found for other Tb^{3+}-containing glasses, such as silicate, phosphate, borate, and borogermanate glasses [15]. The largest Verdet constant reported thus far for Tb^{3+}-containing glasses is 185 rad/T m for $40Tb_2O_3$-$10Dy_2O_3$-$16.67B_2O_3$-$10Ga_2O_3$-$10SiO_2$-$3.33P_2O_5$ glass [14], but the present glasses exhibit larger Verdet constants; the largest value, i.e., 234 rad/T m, was observed for the 60T glass.

It is well known for glasses containing rare-earth ions that the relationship between the Verdet constant, V, and the wavelength, λ, is represented with a single-oscillator model based on the Van Vleck-Hebb theory [23], and is expressed as:

$$V^{-1} = \frac{g\mu_B ch}{4\pi^2 \chi C_t}\left(1 - \frac{\lambda^2}{{\lambda_t}^2}\right), \qquad (1)$$

where g is the Landé g-factor, μ_B is the Bohr magneton, c is the velocity of light, h is the Planck constant, χ is the magnetic susceptibility, C_t is the effective transition probability, and λ_t is the effective transition wavelength. The

relationship between the magnitude of the inverse Verdet constant and the square of the wavelength is illustrated for the present glasses and the TGG single crystal in Fig. 4. A linear relationship is observed for all the samples. We can evaluate λ_t from the intersection of the linear V^{-1}-λ^2 relation with the λ^2 axis. The values of λ_t are listed in Table 1. It is known that λ_t is usually close to the 4f-5d transition energy of the rare-earth ion. For the case of the Tb^{3+} ion, λ_t is approximately 250 nm, corresponding to the $4f^8 \Leftrightarrow 4f^75d$ transition [14]. In the present glass samples, λ_t increases with increasing Tb_2O_3 concentration, and these λ_t values are reasonable for the 4f-5d transition of the Tb^{3+} ion. Optical absorption spectra are shown in Fig. 5. The UV absorption edge due to the $4f^8 \Leftrightarrow 4f^75d$ transition also shifts towards the higher wavelength side with increasing Tb_2O_3 concentration, consistent with the dependence of λ_t on the Tb_2O_3 concentration.

From the Faraday rotation angle and absorbance, the magneto-optical figure of merit (FoM) can be estimated by

$$\mathrm{FoM} = \theta_F/A, \qquad (2)$$

where A is the absorbance. FoM as a function of wavelength is shown in Fig. 6. The values of FoM illustrated in Fig. 6 were obtained under an external magnetic field of 1 T. The values of FoM at 633 nm are also listed in Table 1. Here, the absorption coefficient includes the contribution from the reflection of incident light at the glass surface.

Although FoM exhibits a sharp dip at ~480 nm, as shown in Fig. 6, it tends to increase with decreasing wavelength. The sharp dip at ~480 nm stems from the absorption due to the f-f transitions of Tb^{3+}. As a whole, the wavelength dependence of FoM is very similar to the wavelength variation of the Verdet constant shown in Fig. 2. Note that the FoM of 60T at 633 nm is approximately 1.7 times larger than that of the TGG single crystal.

Gao et al. [15] reported the Verdet constant and FoM for GeO_2-B_2O_3-Al_2O_3-Ga_2O_3 glasses heavily doped with Tb^{3+}. For their glasses, the magnitude of Verdet constant increased with increasing Tb^{3+} content, but the absorption coefficient in the visible region also increased, presumably because of the absorption by Tb^{4+}. In consequence, FoM increases, becomes maximum, and decreases in the visible region as the concentration of Tb ions increases. In contrast, the valence state of terbium ions in the present glasses is mainly trivalent, which was achieved by the annealing in H_2/N_2 atmosphere. As a consequence, the present glasses exhibit low absorption coefficients, leading to the large FoM. Note that the transmittance of the glasses

includes the effect of reflection, that is to say, the FoM presented here is the minimum value expected for the glasses.

Recently, Nakatsuka et al. [24] prepared superparamagnetic FeO-SiO_2 vitreous films, and revealed that its Faraday effect was 4110 rad m^{-1} at 633 nm. This value is approximately 20 times larger than the present 60T glass and the largest among all of the glassy materials as well. However, the vitreous FeO-SiO_2 films have somewhat intense absorption in the short wavelength region, in particular, at wavelengths shorter than 500 nm or so. This is a disadvantageous point when the material is applied to a short-wavelength Faraday rotator. In contrast, the present glasses show quite low absorption coefficient in such a short wavelength region, so that they can be applied to many kinds of devices, such as an optical isolator for high power and short wavelength laser.

4. Conclusion

Borate glasses containing a high content of Tb^{3+} ions were prepared by containerless processing. The glasses exhibited fairly large Veldet constants from 172 to 234 rad/T m at 633 nm; these values are larger than that of the TGG single crystal. Furthermore, the glasses had low optical absorption coefficients in the vis-NIR region. Consequently, fairly large FoM was achieved; ~1.7 times larger than that of the TGG single crystal. This fact indicates that these glasses are promising materials for application to optical isolators for vis-NIR lasers. Considering that we can fabricate glass materials with various shapes, we believe that these present glasses have a great potential for the development of new magneto-optical devices.

References

[1] J. F. Dillon Jr., J. Appl. Phys. **39** (1968) 922-929

[2] T. Okuda, N. Koshizuka, K. Hayashi, H. Taniguchi, K. Satoh, and H. Yamamoto, IEEE Trans. J. Magn. Jpn. **3** (1988) 483-484

[3] A. Thavendrarajah, M. Pardavi-Horvath, and P. E. Wigen, IEEE Trans. Magn. **25** (1989) 4015-4017

[4] S. Mino, M. Matsuoka, A. Shibukawa, and K. Ono, Jpn. J. Appl. Phys. **29** (1990) L1823-L1825

[5] B. M. Simion, G. Thomas, R. Ramesh, V. G. Keramidas, and R. L. Pfeffer, Appl. Phys. Lett. **66** (1995) 830-832

[6] N. Adachi and T. Ota, J. Ceram. Soc. Jpn. **122** (2014) 40-43
[7] D. J. Dentz, R. C. Puttbach, and R. F. Belt, AIP Conf. Proc. **18** (1974) 954-958
[8] M. W. Shafer, and J. C. Suits, J. Am. Ceram. Soc. **49** (1966) 261-264
[9] K. Tanaka, K. Fujita, N. Soga, J. Qiu, and K. Hirao, J. Appl. Phys. **82** (1997) 840-844
[10] H. Akamatsu, K. Fujita, Y. Nakatsuka, S. Murai, and K. Tanaka, Opt. Mater. **35** (2013) 1997-2000
[11] K. Tanaka, T. Ohyagi, K. Hirao, N. Soga, and H. Mori, Glastech. Ber. **65** (1992) 267-269
[12] K. Tanaka, K. Hirao, and N. Soga, Jpn. J. Appl. Phys. **34** (1995) 4825-4826
[13] J. Qiu, K. Tanaka, N. Sugimoto, and K. Hirao, J. Non Cryst. Solids **213&214** (1997) 193-198
[14] T. Hayakawa, M. Nogami, N. Nishii, and N. Sawanobori, Chem. Mater. **14** (2002) 3223-3225
[15] G. Gao, A. Winterstein-Beckmann, O. Surzhenko, C. Dubs, J. Dellith, M. A. Schmidt, and L. Wondraczek, Sci. Rep. **5**, (2015) 8942
[16] Z. X. Mo, H. W. Guo, P. Liu, Y. D. Shen, and D. N. Gao, J. Alloys Comp. **658** (2016) 967-972
[17] H. Guo, Y. Wang, Y. Gong, H. Yin, Z. Mo, Y. Tang, and L. Chi, J. Alloys Comp. **686** (2016) 635-640
[18] J. Yu, Y. Arai, T. Masaki, T. Ishikawa, S. Yoda, S. Kohara, H. Taniguchi, M. Itoh, and Y. Kuroiwa, Chem. Mater. **18** (2006) 2169-2173
[19] M. Kaneko, J. Yu, A. Masuno, H. Inoue, M. S. V. Kumar, O. Odawara, and S. Yoda, J. Am. Ceram. Soc., **95** (2012) 79-81
[20] A. Masuno, and H. Inoue, Appl. Phys. Exp. **3**, (2010) 102601
[21] K. Yoshimoto, A. Masuno, H. Inoue, and Y. Watanabe, J. Am. Ceram. Soc. **95** (2012) 3501-3504
[22] A. D. Sontakke, and K. Annapurna, Spectrochim. Acta Part A **94** (2012) 180-185
[23] J. H. Van Vleck and M. H. Hebb, Phys. Rev. **46** (1934) 17-32
[24] Y. Nakatsuka, K. Pollok, T. Wieduwilt, F. Langenhorst, M. A. Schmidt, K. Fujita, S. Murai, K. Tanaka and L. Wondraczek, Adv. Sci. **4** (2017) 1600299

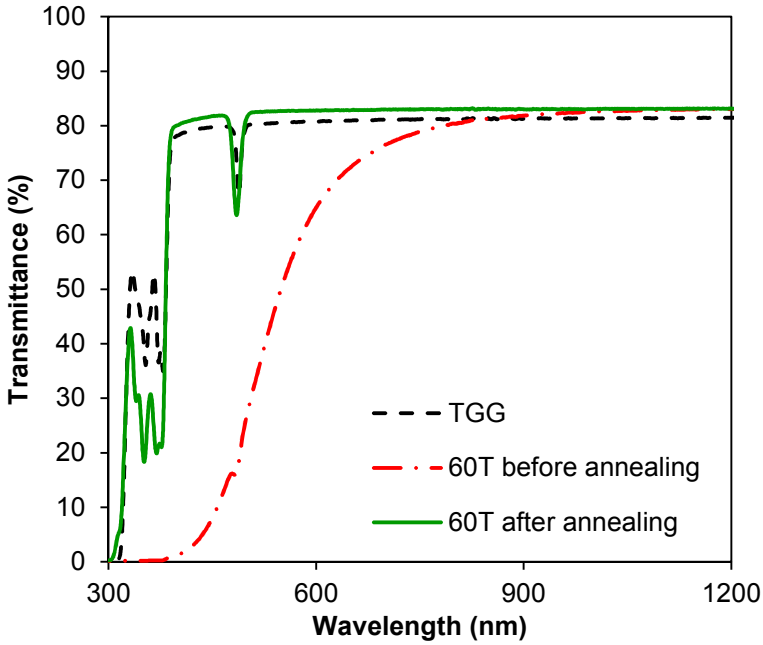

Figure 1. Transmittance spectra of 60T before annealing, 60T after annealing, and $Tb_3Ga_5O_{12}$ (TGG).

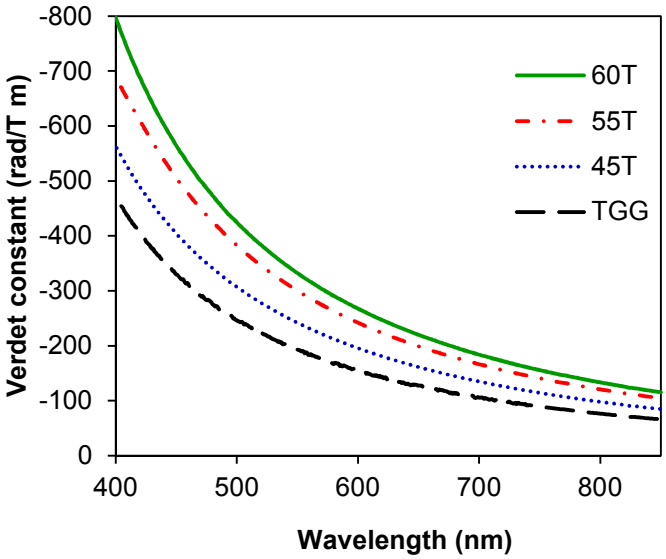

Figure 2. Variation of Verdet constant with wavelength for 45T, 55T, 60T, and TGG at room temperature.

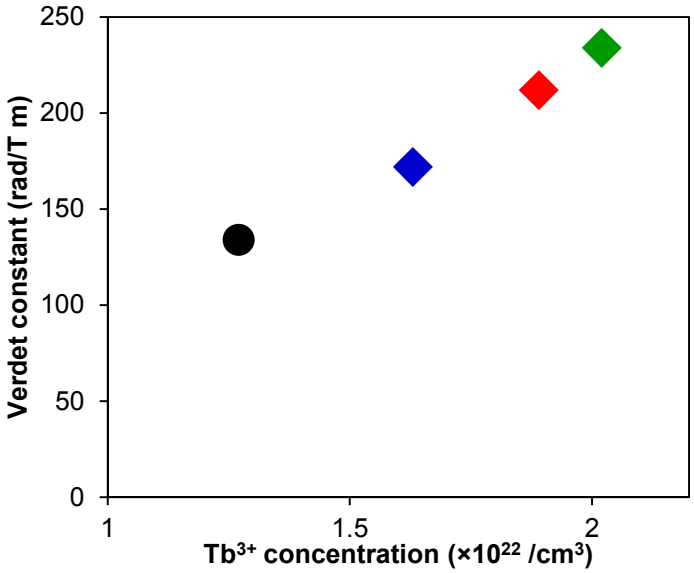

Figure 3. Dependence of Verdet constant on Tb^{3+} ion concentration at a wavelength of 633 nm.

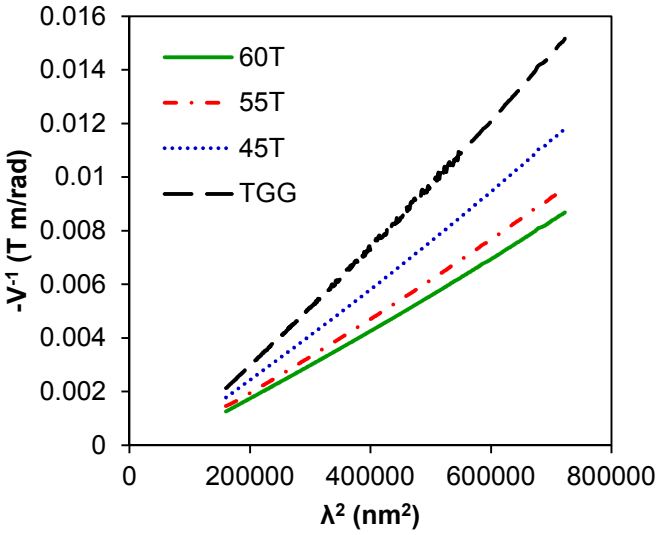

Figure 4. Relationship between the inverse Verdet constant (V^{-1}) and square of wavelength of incident light (λ^2).

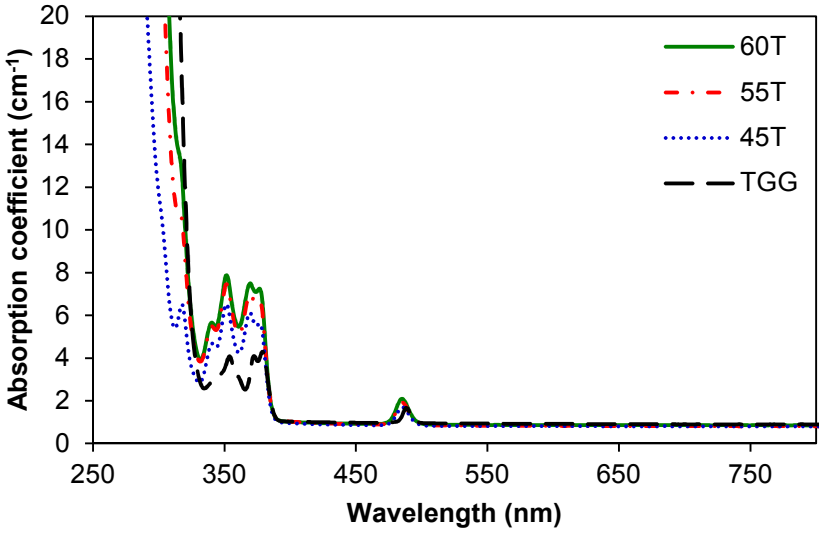

Figure 5. Optical absorption spectra of 45T, 55T, 60T, and TGG.

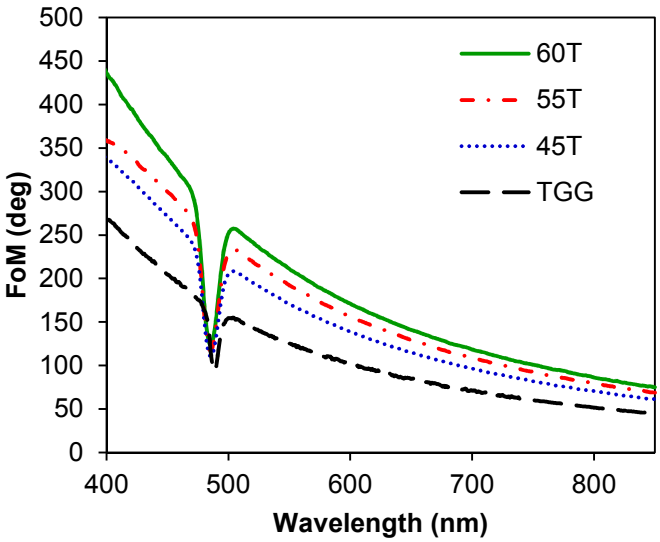

Figure 6. Wavelength dependences of FoM for 45T, 55T, 60T, and TGG. The external magnetic field was 1 T.

Table 1 Glass transition temperature (T_g), crystallization temperature (T_c), density, Tb^{3+} ion concentration, Verdet constant at 633 nm, effective transition wavelength (λ_t), and FoM at 633 nm (external magnetic field of 1 T) for the 45T, 55T, and 60T glasses as well as single-crystalline TGG.

Samples	45T	55T	60T	TGG
T_g (°C)	784	784	803	
T_c (°C)	887	863	861	
Density (g/cm^3)	6.15	6.7	6.9	7.13
Tb^{3+} concentration (×10^{22} /cm^3)	1.67	1.89	2.02	1.27
Verdet constant at 633 nm (rad/T m)	172	212	234	134
λ_t (nm)	260	264	267	275
FoM at 633 nm (deg)	122	138	150	90